## Title

microRNA-17–92 Regulates IL-10 Production by Regulatory T Cells and Control of Experimental Autoimmune Encephalomyelitis



## Journal

The Journal of Immunology, 191(4)

## ISSN

0022-1767

## Authors

de Kouchkovsky, Dimitri
Esensten, Jonathan H
Rosenthal, Wendy L
et al.

## Publication Date

2013-08-15

## DOI

10.4049/jimmunol.1203567

Peer reviewed

This information is current as of July 16, 2013.

# microRNA-17–92 Regulates IL-10 Production by Regulatory T Cells and Control of Experimental Autoimmune Encephalomyelitis

Dimitri de Kouchkovsky, Jonathan H. Esensten, Wendy L. Rosenthal, Malika M. Morar, Jeffrey A. Bluestone and Lukas T. Jeker

*J Immunol* published online 15 July 2013
http://www.jimmunol.org/content/early/2013/07/13/jimmunol.1203567



*The Journal of Immunology* is published twice each month by The American Association of Immunologists, Inc., 9650 Rockville Pike, Bethesda, MD 20814-3994.

Print ISSN: 0022-1767 Online ISSN: 1550-6606.

Published July 15, 2013, doi:10.4049/jimmunol.1203567



# microRNA-17–92 Regulates IL-10 Production by Regulatory T Cells and Control of Experimental Autoimmune Encephalomyelitis

**Dimitri de Kouchkovsky,* Jonathan H. Esensten,* Wendy L. Rosenthal,* Malika M. Morar,* Jeffrey A. Bluestone,*,†,[1] and Lukas T. Jeker*,†,[1]**

**microRNAs (miRNA) are essential for regulatory T cell (Treg) function but little is known about the functional relevance of individual miRNA loci. We identified the miR-17–92 cluster as CD28 costimulation dependent, suggesting that it may be key for Treg development and function. Although overall immune homeostasis was maintained in mice with miR-17–92–deficient Tregs, expression of the miR-17–92 miRNA cluster was critical for Treg accumulation and function during an acute organ-specific autoimmune disease in vivo. Treg-specific loss of miR-17–92 expression resulted in exacerbated experimental autoimmune encephalitis and failure to establish clinical remission. Using peptide-MHC tetramers, we demonstrate that the miR-17–92 cluster was specifically required for the accumulation of activated Ag-specific Treg and for differentiation into IL-10–producing effector Treg.** ***The Journal of Immunology*****, 2013, 191: 000–000.**

Regulatory T cells (Treg) are essential for systemic immune homeostasis. However, despite over a decade of intense research, the molecular understanding of Treg function during active immune and autoimmune responses is still incomplete. microRNAs (miRNAs) are important posttranscriptional regulators of gene expression that form an integral component of cellular biology. Treg-specific ablation of key genes of miRNA biogenesis including *Dicer* (1–3), *Drosha* (2), and *Dgcr8* (4) leads to a scurfy-like syndrome illustrating that global expression of miRNAs is essential for Treg-mediated immune homeostasis. Yet, the role of individual miRNAs in Treg function is largely unresolved (5).

The miR-17–92 miRNA cluster is transcribed as a polycistronic primary transcript encoding six miRNAs from four different seed families (miR-17, miR-18a, miR-19a, miR-20a, miR-19b, and miR-92). Two paralog miRNA clusters (miR-106a–363 and miR-106b–25) differ from the miR-17–92 cluster in their number of miRNAs. Oncogenic properties of miR-17–92 have been well documented (6), and more recently, miR-17–92 was found to be physiologically relevant for lung, heart, and skeletal development (7–9). miR-17–92–deficient mice display impaired B cell development but have normal T cell numbers (7). However, miR-17–92 promotes T cell survival and efficient Th1 responses, regulates CD8 effector versus memory differentiation, and inhibits TGF-β–induced in vitro differentiation into induced Tregs (10, 11). miR-17–92 is induced upon T cell activation, but the functional relevance of this upregulation and its inductive signals have not been addressed (12, 13). Transgenic (Tg) miR-17–92 overexpression in T and B cells was sufficient for the development of lymphoproliferative disease and autoimmunity, but the underlying mechanisms of the autoimmunity remain obscure (14). T cells from miR-17–92 Tg mice displayed mildly increased proliferative capacity and survival, possibly through phosphatase and tensin homolog deleted on chromosome 10 (*Pten*) and BCL-2–interacting mediator of cell death (*Bim*) repression (14). Of note, members of the miR-17–92 cluster are dysregulated in peripheral blood specimens from multiple sclerosis (MS) patients (15, 16).

T cell activation requires binding of the TCR to its cognate peptide presented on MHC molecules by APCs. APCs provide a second signal called costimulation to allow full activation. The prototypical costimulatory molecule is CD28, which binds to its receptors CD80 and CD86. T cell costimulation equips cells with properties necessary to cope with the specific activation-induced stress response (17), enabling the cells to survive and undergo

*Diabetes Center and Department of Medicine, University of California, San Francisco, CA 94143; and †Department of Pathology, University of California, San Francisco, San Francisco, CA 94117

[1]J.A.B. and L.T.J. should be considered cosenior authors.

Received for publication January 10, 2013. Accepted for publication June 8, 2013.

This work was supported by National Institutes of Health Grants P01 AI35297 and U19 AI056388 (to J.A.B.) and P30 DK63720 (for core support) and a scholar award from the Juvenile Diabetes Research Foundation (to J.A.B.). J.A.B. is an A.W. and Mary Margaret Clausen Distinguished Professor. L.T.J. was supported by the Swiss National Science Foundation (Grant PBBSB-118644) and the Swiss Foundation for Grants in Biology and Medicine/Swiss National Science Foundation (Grant PASMP3-124274/1).

J.H.E., J.A.B., and D.d.K. initiated the study; J.H.E., D.d.K., and L.T.J. designed and performed experiments; W.L.R. and M.M.M. performed experiments; J.A.B. provided financial resources and infrastructure; J.H.E. and D.d.K. contributed to writing the manuscript; J.A.B. and L.T.J. designed experiments, oversaw the study, and wrote the manuscript. All authors had access to primary data and approved the final manuscript.

The microarray data presented in this article have been submitted to the Gene Expression Omnibus (http://www.ncbi.nlm.nih.gov/geo/) under accession number GSE36071.

Address correspondence and reprint requests to Drs. Jeffrey A. Bluestone or Lukas T. Jeker, Executive Vice Chancellor and Provost, University of California, S-115 Box 0400, 513 Parnassus Avenue, San Francisco, CA 94141-0540 (J.A.B.) or Assistant Adjunct Professor, University of California San Francisco Diabetes Center and Department of Pathology, University of California, Box 0540, 513 Parnassus Avenue, San Francisco, CA 94143-0540 (L.T.J.). E-mail addresses: Jeff.bluestone@ucsf.edu (J.A.B.) or ljeker@diabetes.ucsf.edu (L.T.J.)

The online version of this article contains supplemental material.

Abbreviations used in this article: BIM, BCL-2–interacting mediator of cell death; EAE, experimental autoimmune encephalitis; KO, knockout; LN, lymph node; MFI, mean fluorescence intensity; MGI, Mouse Genome Informatics; miRNA, microRNA; MOG, myelin oligodendrocyte glycoprotein; PTEN, phosphatase and tensin homolog deleted on chromosome 10; Spl, spleen; Tconv, conventional T cell; Teff, effector T cell; Tg, transgenic; Treg, regulatory T cell; UCSF, University of California San Francisco.

clonal expansion. Thus, triggering of CD28 induces metabolic changes (18) and enhances survival and proliferation (19).

We have previously demonstrated that CD28-mediated costimulation was an intrinsic requirement for Treg development and function. CD28 engagement is particularly important for thymic development and peripheral survival of Tregs. CD28-deficient or CTLA-4Ig–treated mice have a marked reduction of $CD4^+CD25^+$ $Foxp3^+$ Tregs (20), and on a susceptible genetic background, these mice develop accelerated diabetes (21). Because Tregs do not produce IL-2, the results suggested that the requirement for CD28 was related to the metabolic and survival functions of this pathway. It is well established that CD28 triggering induces a specific gene expression signature including upregulation of prosurvival genes (*Bcl-$x_L$* and *Bcl-2*), downregulation of proapoptotic genes (e.g., *Bim*), differential expression of transcription factors, and upregulation of cytokine receptors such as the IL-2Rα-chain (CD25) that further enhance survival and proliferation (19). In part, this is achieved through enhancement of PI3K signals by CD28-mediated inhibition of the PI3K inhibitor PTEN (22).

Finally, a multitude of mechanisms have been postulated to explain Treg-suppressive activity (23). The emerging view is that Treg integrate environmental cues leading to phenotypic and functional diversification through induction of various transcription factors. Thus, subsets of Treg may use different cell surface molecules and soluble factors to suppress immunity depending on their microenvironment. One of the suppressive mechanisms, production of the inhibitory cytokine IL-10 by $Foxp3^+$ Treg, plays a limited physiologic role in systemic homeostasis and mainly affects Treg function in mucosal tissues (24). In contrast, solid evidence demonstrates that IL-10 produced by Tregs plays an important role in controlling experimental autoimmune encephalitis (EAE), a murine model of multiple sclerosis. Importantly, adoptively transferred IL-10–deficient Tregs cannot prevent EAE (25).

In summary, Tregs are highly costimulation dependent, and miRNAs are essential for Treg function. These two complementary research areas led to the study of CD28-regulated miRNAs in Treg biology. Using a combination of miRNA microarray, conditional gene disruption, and tetramer technology, we found that miR-17–92 is upregulated by CD28-mediated costimulation and is required for IL-10 production and the accumulation of Ag-specific Tregs in EAE, a concept with potentially important diagnostic and/or therapeutic implications.

## Materials and Methods

### *Human blood*

Whole blood was obtained via venipuncture from healthy adult volunteers (males, age range: 19–29). Blood was collected in sodium heparin–containing Vacutainer tubes (BD Biosciences). PBMCs were isolated using Ficoll–Paque PLUS (Amersham Biosciences), as described previously (26).

### *Isolation and activation of human $CD4^+CD45RA^+$ T cells*

For microarray analysis, $CD4^+CD45RA^+$ T cells were isolated on a BD FACSAria II cell sorter (BD Biosciences) using anti-CD4 (clone SK3; BD Biosciences) and CD45RA (clone HI100; BD Biosciences). Cells with >99% purity were seeded at a density of $1 \times 10^6$ cells/ml RPMI 1640 medium supplemented with 5% human heat-inactivated pooled AB serum (Valley Biomedical). Cells were activated with latex beads conjugated to control Ab (clone MPC-11; BD Biosciences) or Abs specific for anti-CD3 (clone OKT3) or to both anti-CD3 and anti-CD28 (clone 9.3). Activation was confirmed by flow cytometry on a BD Biosciences FACSCalibur using anti-CD25 (clone 2A3; BD Biosciences) and anti-CD69 (clone L78; BD Biosciences).

### *Flow cytometry*

Flow cytometry and fluorescence activated cell sorting was performed as described previously (1). Live/dead discrimination was done using Live/Dead Fixable Violet Dead Cell Staining kit, according to the manufacturer's recommendations (Invitrogen Life Technologies). For intracellular cytokine staining (IFN-γ [clone XMG1.2], IL-17A [clone eBio 17B7], and IL-10 [clone JES5-16E3]; eBioscience), cells were stimulated for 3 h with 10 ng/ml PMA (Sigma-Aldrich), 0.5 μM ionomycin (Sigma-Aldrich), and 3 μM monensin. IL-10 staining: after viability and surface staining cells were resuspended in 100 μl BD Cytofix (BD Biosciences) and incubated for 15 min at room temperature. After washing, cells were stained for 1 h at room temperature with intracellular Abs diluted in 100 μl Invitrogen Fix & Perm medium B. Cells were then washed with BD Perm/Wash buffer. Anti-Ki67 (clone B56; BD Biosciences) was costained with the Foxp3 staining in Foxp3 Perm buffer (eBioscience). Acquisition was performed uncompensated on a BD LSR II using BD FACSDiva software. Data were then exported as FCS 3.0 for compensation and analysis in FlowJo for Mac (always latest version up to 9.4.10; Tree Star). Normalization for mean fluorescence intensity (MFI) across multiple experiments: the average MFI of control samples was defined as an MFI of 1. All other values were normalized as fold difference to this average.

### *RNA preparation and microarray analysis*

RNA samples for microarray were prepared with TRIzol (Invitrogen) according to the manufacturer's instructions. RNA integrity was confirmed with a Bioanalyzer 2100 (Agilent); only samples with a RIN ≥ 7.5 were processed further. RNA samples for quantitative real-time PCR analysis were extracted using the RNAeasy kit (Qiagen) using the manufacturer's recommended protocol. The miRNA microarrays were miRCURY LNA microRNA arrays (Exiqon). miRNA array labeling, hybridization and scanning were performed at the University of California San Francisco (UCSF) Gladstone Genomics Core. Array data were analyzed using GeneSpring GX software (Agilent). Raw data are available at Gene Expression Omnibus (http://www.ncbi.nlm.nih.gov/geo/) with accession number GSE36071.

### *Quantitative real-time PCR*

For miRNAs, RNA was reverse transcribed using the TaqMan MicroRNA Reverse Transcription Kit (Applied Biosystems) following the manufacturer's instructions. The reverse and forward primers as well as the probes used in this step were designed as previously described (27) and obtained from Integrated DNA Technologies. Sequences can be found at http://urology.ucsf.edu/blellochlab/protocols/miRNAqPCRsequences.txt. The controls for the human and mouse samples were the small RNAs RNU24 and Sno234, respectively (Applied Biosystems).

For mRNAs RNA was reverse transcribed using the High Capacity cDNA Reverse Transcription Kit (Applied Biosystems). A *Dgcr8* primer/probe kit was from Applied Biosystems. cDNAs were amplified with TaqMan Fast Real-Time PCR Universal Master Mix (2×), no AmpErase UNG (Applied Biosystems) in the cycler system 7500 Fast Real-Time PCR system (Applied Biosystems).

### *Mice*

Conditional miR-17–92lox mice (7) were obtained from The Jackson Laboratory (Bar Harbor, ME). Foxp3-GFP-cre1$a^{hi}$ (Mouse Genome Informatics [MGI], http://www.informatics.jax.org/: 4430213) (1), *Pten* lox (MGI: 3819698) (28), and *Bim* knockout (KO) (MGI: 2156498) (29) mice have been described previously. Mice were on a genetically mixed background crossed to B6.miR-17–92lox to have at least 50% H-$2^b$.

### *Isolation of mouse T cells*

Single-cell suspensions were obtained from the spleen (Spl) and lymph nodes (LNs) of euthanized mice. Cells were washed and filtered before being sorted on a Moflo (DakoCytomation) for $CD4^+CD62L^+$ cells and $CD4^+CD62L^+Foxp3\text{-}GFP^+$ cells, as described previously (30). Cells were activated with plate-bound anti-mouse CD3 (clone 145-2C11) with or without anti-mouse CD28 (clone PV-1).

### *EAE induction*

EAE was induced as described previously (31). Briefly, 200 μg myelin oligodendrocyte glycoprotein $(MOG)_{35–55}$ peptide (Genemed Synthesis) emulsified in CFA (Sigma-Aldrich) was injected s.c. in each mouse. Mice were injected i.p. with pertussis toxin (400 ng/dose; List Biological Labs) on days 0 and 2 after immunization.

### *Tetramer staining and pulldown*

APC-labeled mouse I-$A^b$ myelin oligodendrocyte glycoprotein peptide 38–49 (GWYRSPFSRVVH) and I-$A^b$ human class II–associated invariant

chain peptide 103–117 (PVSKMRMATPLLMQA) as a negative control to set gates were from the Emory National Institutes of Health Tetramer Facility (http://tetramer.yerkes.emory.edu/). MOG Tetramer staining and enrichment were done as described previously (32).

### *Lymphocyte isolation from CNS*

Isolation of lymphocytes from the CNS was performed following a protocol modified from Ref. 33. Briefly, anesthetized mice were perfused with ice-cold PBS through the left cardiac ventricle until the effluent ran clear. Spinal cord was blown out using hydrostatic pressure, and cerebellum and brain stem were dissected, cut into pieces, and then digested at 37˚C for 30 min with 320 U/ml collagenase D (Roche) and 50 μg/ml DNase I (Roche). Cells were separated from myelin by passing the digestion mix through a 40-μm Nytex strainer followed by a Percoll gradient (30/70%) (Amersham Biosciences). Mononuclear cells were removed from the interphase, washed, and resuspended in staining buffer for flow cytometry or cell culture media for restimulation.

### *Statistics*

For statistical analysis Prism 5.0 (GraphPad Software) was used. $*p \leq 0.05$, $**p \leq 0.01$, $***p \leq 0.001$, and $****p \leq 0.0001$. Differences between groups were considered statistically significant if the null hypothesis was rejected by a $p$ value of ≤5%. No data points were excluded from the analysis unless specified otherwise.

### *Study approval*

*Human blood.* Informed written consent from healthy blood donors was obtained in accordance with the reviewed and approved policies and procedures at UCSF. Ethics approval was granted by the UCSF Institutional Review Board (approval number H7023-22712-08).

*Mice.* Mice used for all experiments were housed and bred under specific pathogen-free conditions in the Animal Barrier Facility of the UCSF Animal Barrier Facility. All animal experiments were approved by the Institutional Animal Care and Use Committee of UCSF (approval numbers AN083988-01 and AN082188-02).

## Results

### *miR-17–92 is part of the CD28 costimulatory network*

CD28 costimulatory signals and miRNAs are both critical for Treg function, but their interconnectivity has not been investigated in Tregs. To study whether miRNAs are involved in T cell costimulation/activation, we generated a miRNA expression signature from purified human naive conventional $CD4^+$ T cells stimulated with anti-CD3 alone or anti-CD3 and anti-CD28 (Supplemental Fig. 1). As previously reported, miR-155 was strongly upregulated after maximal activation with the combination of TCR/CD3 and CD28 stimulus. However, the majority of the upregulated miRNAs were encoded by only three gene loci, all members of the miR-17–92 cluster and its paralogs. Quantitative PCR analysis confirmed miR-17 upregulation (data not shown). To investigate the functional relevance of CD28-mediated miR-17–92 upregulation, we turned our attention to murine T cells because of the availability of a conditional gene ablation mouse model allowing a thorough in vivo analysis (7). miR-17, which is a unique representative miRNA of the miR-17–92 cluster, was markedly upregulated in mouse naive $CD4^+$ T cell samples stimulated with the combination of anti-CD3 and anti-CD28 (Fig. 1A). miR-155 induction followed a similar CD28-dependent pattern. We observed low-level induction of both miR-17–92 and miR-155 in some samples stimulated with anti-CD3 alone. Kinetic analyses of miR-17 expression showed no change at 6 h poststimulation, but upregulation was detected by 12 h poststimulation and further increased at 24 h when stimulated with the combination of anti-CD3 and anti-CD28 (Fig. 1B). In addition, we examined the expression of miR-17 specifically in the highly CD28 costimulation–dependent Treg subset. As in conventional T cells (Tconvs), anti-CD3 stimulation alone neither induced miR-17 nor miR-155 (Fig. 1C). In contrast, combined anti-CD3 and CD28 triggering induced

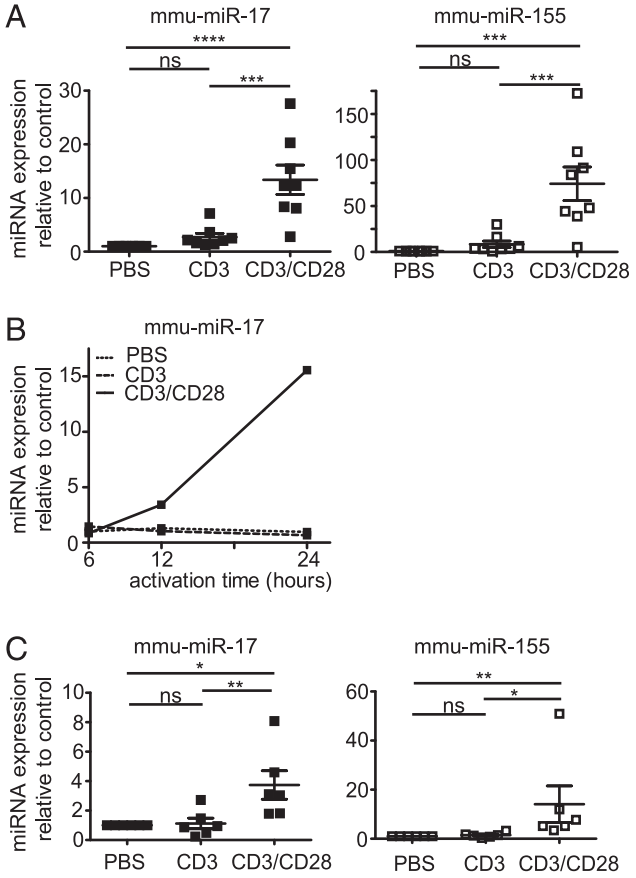


**FIGURE 1.** miR-17–92 is part of the CD28 costimulatory network. (**A**) Mouse miR-17 and miR-155 expression in purified Tconvs stimulated for 24 h with PBS, anti-CD3 (CD3) or a combination of anti-CD3 and antiCD28 (CD3/CD28), presented relative to sno234 and normalized to PBS. (**B**) Quantitative PCR time-course analysis of murine miR-17 expression relative to sno234. (**C**) Quantitative PCR on RNA from naive murine $CD4^+CD25^+CD62L^{hi}$ Tregs activated with the indicated conditions for 24 h in vitro. Data are pooled from four (A), one (B), and four (C) experiments with a total of eight individual mice (A), two mice (B), and six individual mice (C), respectively; individual dots represent cells derived from individual mice. (A) One-way ANOVA with a post hoc Bonferroni multiple comparison test: $p < 0.0001$ (miR-17); $p = 0.0001$ (miR-155). (C) Kruskal–Wallis test with post hoc Dunn's multiple comparison test: $p = 0.0045$ (miR-17) and $p = 0.0022$ (miR-155).

miR-17 as well as miR-155 (Fig. 1C). We note that the relative induction of both miRNAs was smaller in Tregs than Tconvs. Because both cell types were activated using the same conditions, this most likely reflects the reduced activation potential of Foxp3 expressing Treg in vitro.

Mice with a T cell-specific lack of miR-17–92 had normal numbers of Tconvs and Tregs and remained healthy as reported previously (D. de Kouchkovsky, J.A. Bluestone, and L.T. Jeker, unpublished observations) (10). In contrast to Jiang et al. (10), we only observed a minor proliferative disadvantage when the anti-CD28 signal was titrated but not with strong activation signals (34). Thus, miR-17–92 miRNAs are part of the costimulatory network and are necessary for optimal CD28 costimulation and maximal T cell activation under certain conditions.

### *Treg-specific miR-17–92 deficiency does not affect immune homeostasis*

To investigate the function of miR-17–92 in Treg in vivo, we crossed the conditional miR-17–92 mice to Foxp3-GFP-hCre Tg mice (1). These mice, designated $Treg^{miR\text{-}17\text{–}92-/-}$, developed

normally, bred, and remained healthy up to 12 mo of age (data not shown). Aged Treg$^{miR\text{-}17\text{–}92-/-}$ mice had Treg frequencies and Foxp3 expression in LNs and Spl comparable to control littermates (Fig. 2A) and did not show any increase in activated CD4$^+$ Foxp3$^-$CD44$^+$CD62L$^{lo}$ cells (Fig. 2B). Thus, in contrast to ablation of all miRNAs, the miR-17–92 cluster is largely dispensable for Tconvs (D. de Kouchkovsky, J.A. Bluestone, and L.T. Jeker, unpublished observations) and Tregs under homeostatic conditions, a finding similar to a previous report (10). This could reflect redundancy of paralog miRNA clusters that compensate for loss of miR-17–92 expression or that the effects of miR-17–92 deletion are only observed under stress conditions with endogenous Ags in vivo. This latter concept is supported by the general agreement that miRNAs are considered fine-tuners of biologic processes forming a protective layer of regulatory elements capable of stabilizing genetic networks under stress (35–38).

*miR-17–92 expression is essential for Treg function during an autoimmune-mediated stress response*

To assess Treg$^{miR\text{-}17\text{–}92-/-}$ function in a disease model that is highly dependent on Tregs, we primed mice with MOG emulsified in CFA to induce EAE. miR-17–92 proved essential to Treg function in this model of acute autoimmune disease because Treg$^{miR\text{-}17\text{–}92-/-}$ mice developed much more severe disease and failed to go into remission compared with control littermates (Fig. 3A, 3B). The clinical disease course strikingly resembled clinical EAE scores of mice with anti–CD25 Ab-mediated Treg depletion (39), indicating that Tregs may be absent or dysfunctional in Treg$^{miR\text{-}17\text{–}92-/-}$ mice. However, although polyclonal Treg frequencies at peak of disease (day 15 postpriming) in CNS isolates were mildly reduced, there was no difference in absolute numbers of Tregs in Treg$^{miR\text{-}17\text{–}92-/-}$ mice compared with control mice (Fig. 3C). Moreover, polyclonal Treg frequencies in control mice inversely correlated with clinical disease (Fig. 3D). Mice with severe disease (clinical scores $\geq$ 3) showed no difference in polyclonal Treg frequency between Treg$^{miR\text{-}17\text{–}92-/-}$ and control mice (Fig. 3E, 3F). Therefore, we hypothesized that either Treg function must have been impaired or that a small subset, perhaps the neural Ag-specific Tregs, were affected by miR-17–92 deficiency.

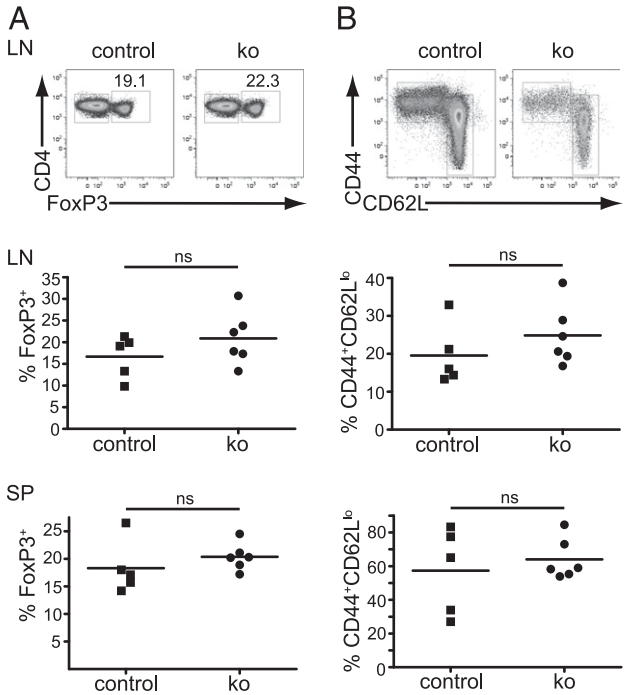


**FIGURE 2.** Treg-specific miR-17–92 deficiency does not affect immune homeostasis. Relative numbers of CD4$^+$Foxp3$^+$ Tregs (**A**) and frequencies of Ag-experienced CD4$^+$CD44$^+$CD62L$^{lo}$ conventional (Foxp3$^-$) T cells (**B**) in 6- to 12-mo-old Foxp3cre.miR-17 92$^{lox/lox}$ and control mice. Representative FACS plots of lymphocytes isolated from LNs (*upper panels*); numbers indicate percentage of cells. Quantification of pooled mice from two independent experiments for LNs and Spl (SP) (A, B; *lower panels*). Two-tailed Mann–Whitney *U* test (A, B). Relative numbers of Foxp3$^+$ Tregs: $p = 0.3602$ (LN); $p = 0.1775$ (SP). Relative numbers of CD44$^+$ CD62L$^{lo}$: $p = 0.2468$ (LN); $p = 0.9307$ (SP). ko, Knockout.

*miR-17–92 preserves Ag-specific Tregs during priming in vivo*

To avoid secondary effects because of inflammation, we studied Treg$^{miR\text{-}17\text{–}92-/-}$ mice at day 7 post-MOG/CFA priming (i.e., before onset of clinical disease) (Fig. 3A). At this time point, pooled LN and Spl cellularity were comparable between control and Treg$^{miR\text{-}17\text{–}92-/-}$ mice (Fig. 4A). We compared the results to mice that were either heterozygous or homozygous for the conditional miR-17–92 allele but lacking the Foxp3-GFP-hCre BAC (designated Cre-) as well as mice carrying the Foxp3-GFP-hCre BAC alone (miR-17–92 wild-type) to exclude artifacts because of the applied cre/loxP technology (40). We did not observe any relevant differences between the two control groups (Fig. 4A, 4B). The frequencies of Foxp3$^+$ Tregs were comparable in control and Treg$^{miR\text{-}17\text{–}92-/-}$ mice (Fig. 4B). Thus, relative and absolute numbers of polyclonal Tregs were comparable at day 7 postpriming (d7) in LNs and Spl and mildly reduced at day 15 in CNS. Next, we investigated whether the increased susceptibility of Treg$^{miR\text{-}17\text{–}92-/-}$ mice to EAE could be a consequence of changes in Ag-specific Treg development. MOG38–49/I-A$^b$ tetramers were used to detect MOG-specific Treg in d7 LN and Spl (Fig. 4C) (32, 33). We could not find any difference in the frequencies of Tconvs or Foxp3$^+$CD25$^+$ Tregs in naive CD4$^+$CD44$^-$tetramer$^-$ T cells or CD4$^+$CD44$^+$tetramer$^-$ T cells (Fig. 4D). In contrast, Treg$^{miR\text{-}17\text{–}92-/-}$ mice had markedly reduced Ag-specific CD4$^+$CD44$^+$tetramer$^+$ Treg/Tconv ratios than control mice (Fig. 4D). This was not due to more conventional T cells (data not shown) but rather reflected reduced absolute numbers of Ag-specific Tregs. miR-17–92–deficient Treg had normal expression of CD127, GITR, CD103, and Neuropilin-1 (Supplemental Fig. 2A–D) but showed a slight reduction of CTLA-4 (Supplemental Fig. 2E). Ag-specific miR-17–92–deficient Tregs upregulated CD25 to the same degree as control Tregs and greater than tetramer$^-$ Tregs (Fig. 4E). These results suggest that tetramer$^+$ Tregs receive a stronger TCR signal and therefore display stronger activation. In this regard, CD69, another activation marker, was increased as well on miR-17–92–deficient Treg (Supplemental Fig. 2F) as previously observed in *Dicer*-deficient CD8$^+$ T cells (41). Bioinformatic analysis predicts multiple miR-17–92 binding sites in the CD69 3′-untranslated region (42), suggesting that the elevated CD69 in Tregs may be due to direct derepression. Taken together, these results suggest that the activation of Treg was not affected by the miR-17–92 deficiency.

*Normal proliferation of miR-17–92–deficient Tregs in vivo*

On the basis of previous reports supporting a physiologic role for miR-17–92 in the enhancement of cell proliferation (14), we took advantage of Ki67 to measure the proliferation of Tregs at d7 postpriming. Naive CD4$^+$CD44$^-$tetramer$^-$ Tconvs and Tregs were all nonproliferating Ki67$^-$ (Fig. 5B). MOG tetramer$^-$ Tconvs and Tregs, expressing an activated CD44$^+$ phenotype, displayed a bimodal Ki67 distribution (with Ki67$^+$ cells representing about half of the cells). These results suggested cellular

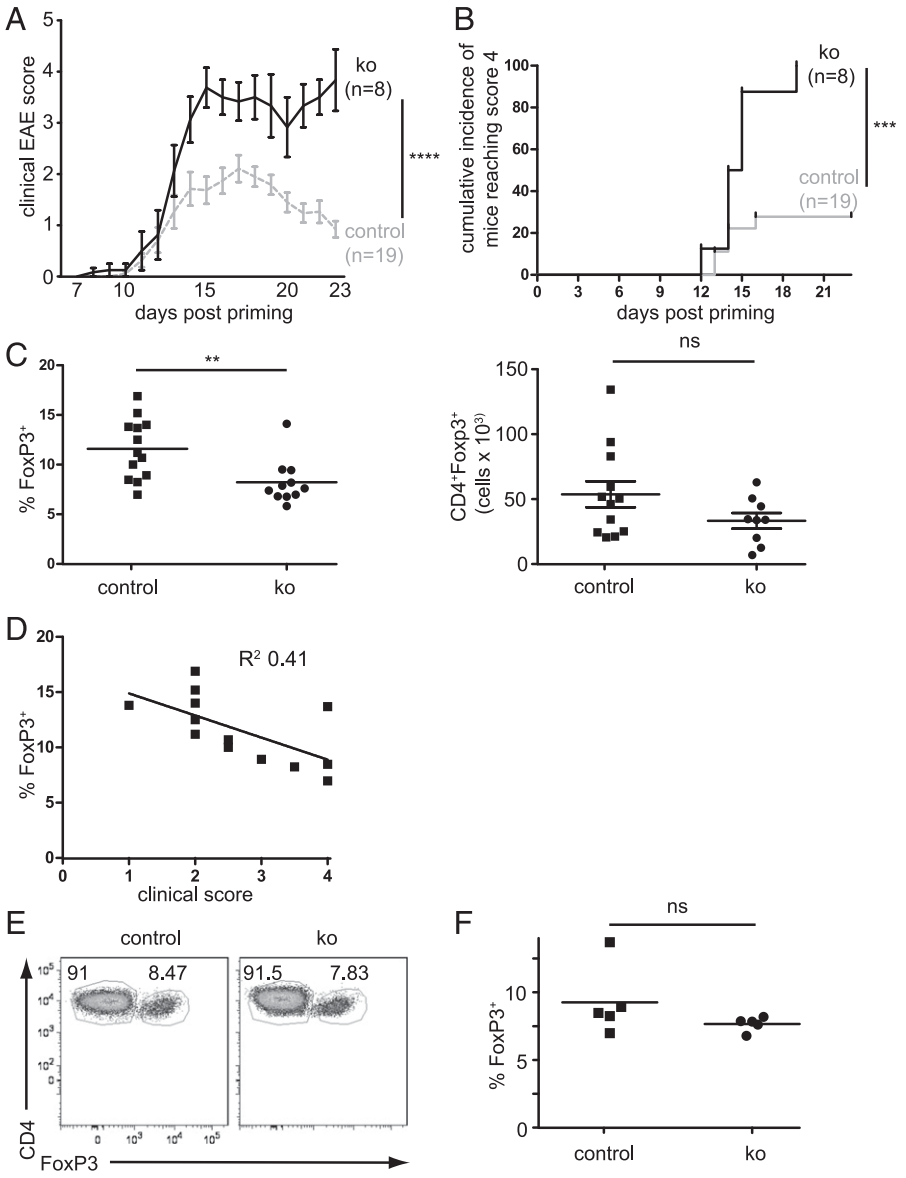


**FIGURE 3.** miR-17–92 expression is essential for Treg function during an autoimmune-mediated stress response. (**A**–**F**) EAE was induced with MOG35–55/CFA in mice with a Treg-specific miR-17–92 deficiency (knockout, "ko") and control mice. (A) Clinical disease scores. (B) Cumulative incidence of mice reaching clinical EAE score 4. (C) Comparison of relative and absolute numbers of polyclonal $CD4^+Foxp3^+$ T cells in CNS isolates from day 15 postpriming in control and ko mice independent on clinical scores. (D) Inverse correlation between clinical EAE score and polyclonal Treg frequency in control mice. (E) Representative FACS plots of lymphocytes isolated from CNS of mice with clinical scores $\geq 3$ at peak of disease (day 15). (F) Quantification of (E). Data are pooled from six independent EAE cohorts with a total of 19 (control) and 8 (ko) mice (A, B) and from five independent cohorts (C–F); individual dots represent cells derived from individual mice. Pooled controls are cre- (miR-17–$92^{wt/wt}$, miR-17–$92^{wt/lox}$, or miR-17–$92^{lox/lox}$) or Foxp3-GFP-hCre.miR-17–$92^{wt/wt}$ mice. $Cre^-$ mice were pooled because we did not observe any obvious differences among the four control groups. Mice with clinical scores $\geq 3$ (E, F) are also included in Fig. 3C. (A) $p < 0.0001$ (two-way ANOVA); (B) $p = 0.0008$ (log-rank [Mantel–Cox] test); (C) $p = 0.02$ (relative number); $p = 0.1658$ (absolute number); (F) $p = 0.0952$ (two-tailed Mann–Whitney); (D) $R^2$: 0.41 (linear regression analysis: deviation from slope zero, $p = 0.0192$).

heterogeneity in these populations perhaps reflecting a small subpopulation of Ag-specific cells not defined by tetramer staining (Fig. 5B). All the $Foxp3^+$ Tregs were $Ki67^+$ among the population of Ag-specific $CD4^+CD44^+$tetramer$^+$ T cells (Fig. 5B, 5C). Because Treg activation and proliferation are normal in the absence of miR-17–92, these results suggest that the reduced number of Ag-specific Tregs (Fig. 4D) likely reflected increased cell death. Thus, in contrast to homeostatic conditions, miR-17–92 deficiency severely and selectively affected Ag-specific Treg accumulation in the inflammatory milieu in vivo.

### *The frequency of miR-17–92–deficient Ag-specific Tregs cannot be rescued by* Pten *deficiency or Bim heterozygosity*

There are a number of gene targets that have been validated as directly miR-17–92 regulated (14). Among them, both PTEN and the proapoptotic molecule, BIM, have been shown to be CD28 costimulation dependent and implicated in T cell activation (22). Therefore, we examined whether one or both of these genes could explain the reduction of tetramer$^+$ miR-17–92–deficient Tregs. To test the importance of miR-17–92–mediated *Pten* repression in Tregs in vivo, we performed genetic rescue experiments. Deleting one or both *Pten* alleles specifically in Tregs did not change overall Treg numbers in the analyzed 6- to 8-wk-old mice, and MOG/CFA priming did not result in a different overall cellularity (data not shown). Similar to data presented in Fig. 4D, frequencies of Ag-specific Tregs were significantly reduced in Treg lacking miR-17–92 compared with control mice confirming our findings in an independent cohort of mice (Fig. 6A). Limiting *Pten* to one allele or deleting it entirely in Tregs did not result in an increased frequency of Ag-specific Treg. Thus, as read out by Ag-specific Treg numbers, *Pten* heterozygosity/deletion was not sufficient to compensate for miR-17–92 deficiency.

IL-2 is essential for Treg survival (43), but eliminating *Bim* can restore Treg numbers in IL-2– or CD25-deficient mice, likely because BIM mediates cytokine deprivation–mediated apoptosis (44, 45). Because conditional *Bim* mice are not available, we immunized $Treg^{miR\text{-}17\text{–}92-/-}$:$Bim^{wt/wt}$,$Treg^{miR\text{-}17\text{–}92-/-}$:$Bim^{wt/-}$ as well as $Bim^{wt/-}$ mice. Germline *Bim* heterozygosity did not increase overall cellularity in our model (data not shown). *Bim* heterozygosity did increase the frequency of Ag-specific Tregs in miR-17–92–sufficient control mice but was not sufficient to rescue miR-17–92 deficiency (Fig. 6B). Thus, although miR-17–92 selectively protects the most vulnerable Ag-specific Tregs during priming, repression of *Pten* and *Bim* heterozygosity on their own

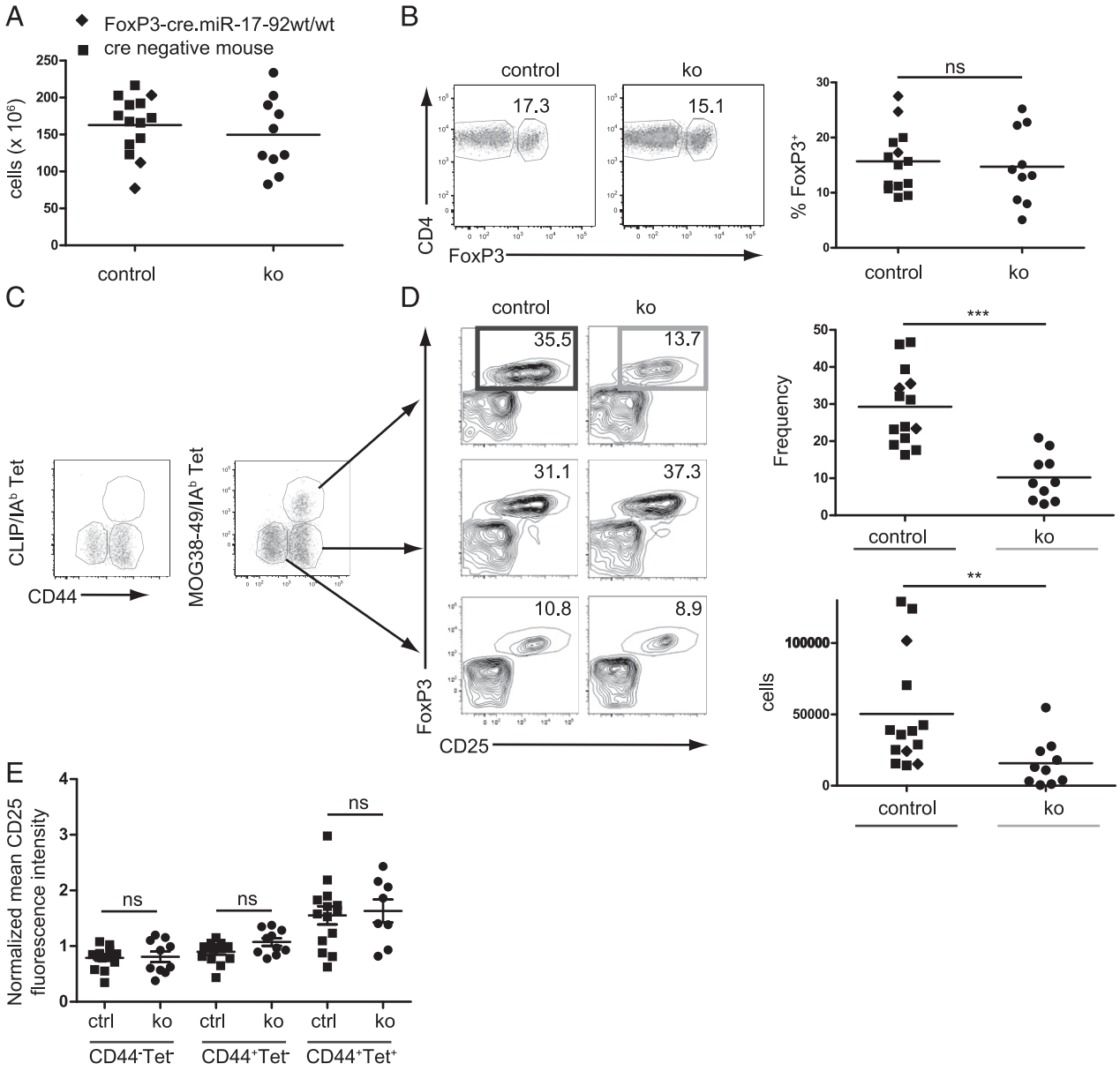


**FIGURE 4.** miR-17–92 preserves Ag-specific Treg during priming in vivo. Pooled LNs and Spl from mice immunized with MOG35–55/CFA were analyzed 7 d postpriming. Data are pooled from four independent experiments. (**A**) Total cellularity of pooled LNs (axillary and inguinal) and Spl. (**B**) Frequency of $CD4^+Foxp3^+$ Tregs. Representative FACS plots (*left panel*) and quantification of pooled data (*right panel*). (**C**) Identification of Ag-specific cells: live singlet $CD8^-B220^-CD11b^-CD11c^-CD4^+$ cells were gated into three populations based on CD44 and MOG38–49/I-$A^b$ tetramer. CLIP/I-$A^b$ tetramer served as negative control. Analysis of frequencies of $Foxp3^+CD25^+$ Tregs for all three populations. (**D**) Representative FACS plots and quantification of relative and absolute numbers of Ag-specific Tregs. Numbers in representative FACS plots indicate percentage of $Foxp3^+CD25^+$ cells. (**E**) Normalized MFI for CD25. The shown control mouse in (D) is a Foxp3-cre1$a^{hi}$.miR-17–$92^{wt/wt}$ mouse to show that the observed phenotype in knockout (ko) mice is not due to cre toxicity. [(D), frequency] $p = 0.0002$ (two-tailed Mann–Whitney); [(D), absolute cell number] $p = 0.0045$ (two-tailed Mann–Whitney).

are likely not sufficient for this protection, suggesting that alternative targets or combinations of targets are functionally relevant.

### *Normal numbers of Ag-specific Tregs in the CNS at peak disease*

To investigate miR-17–92 function in Tregs at the site of inflammation, we examined the effect of Treg-specific miR-17–92 deficiency in the CNS during the peak of the inflammatory response (d15). The number of infiltrating cells was comparable in both groups (Fig. 7A). Moreover, there was no difference in relative or absolute numbers of CNS infiltrating $CD4^+$ T cells between mice with intact or miR-17–92–deficient Tregs (Fig. 7B). Importantly, the overall number of Tregs was not reduced when comparing the total $Foxp3^+$ cells (Fig. 3C–F). Unlike the reduction of Ag-specific Tregs in LNs, there was a significant number of remaining miR-17–92–deficient Tregs in the CNS, both $tetramer^+$ MOG-specific as well as $CD44^+$ activated but MOG-$tetramer^-$ Tregs, which constituted the vast majority of the infiltrating Tregs (Fig. 7C), suggesting that vigorous proliferation (Fig. 5) compensated for the loss of Ag-specific Tregs. Accordingly, the frequency and absolute numbers of $CD4^+IFN\gamma^+IL\text{-}17A^-$ (Th1) and $CD4^+IFN\gamma^-IL\text{-}17A^+$ (Th17) was comparable between the two groups (Fig. 8). Importantly, the presence of substantial Treg numbers in the CNS suggested that the exacerbated disease might be due to more than just a consequence of impaired Treg expan-

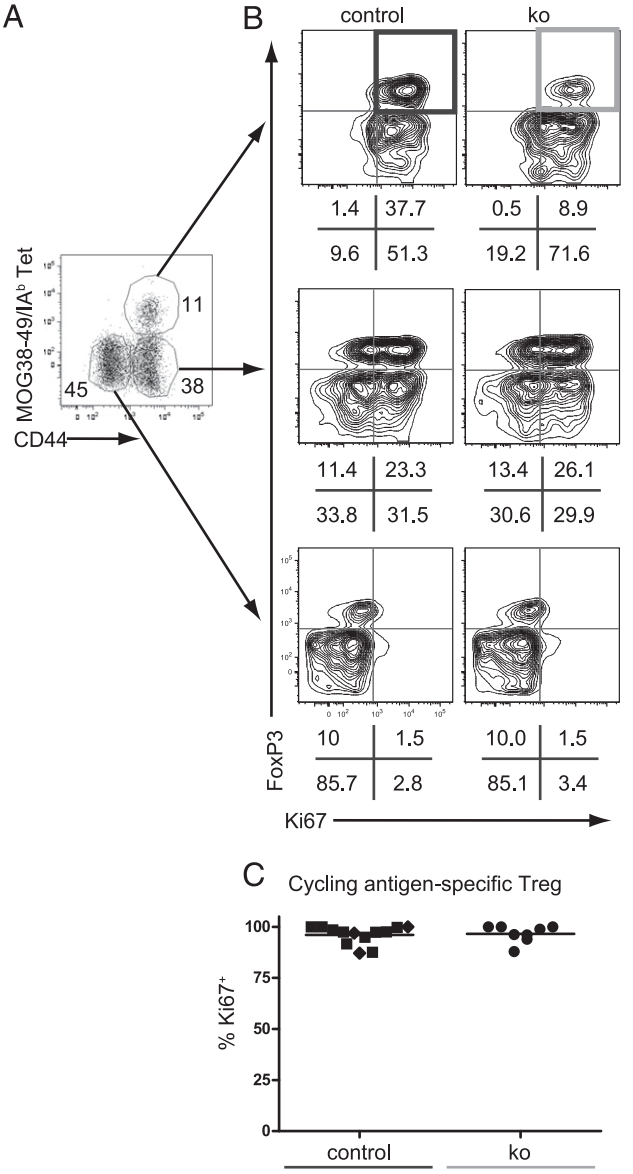


**FIGURE 5.** Normal proliferation of miR-17–92–deficient Treg in vivo. Data are from the same experiments as shown in Fig. 4 but analyzing the proliferation marker, Ki67. (**A**) Gating strategy to define tetramer$^+$ T cells. Numbers indicate the frequencies of cells in each gate for the shown representative graph of the control mouse shown in (**B**). (B) Representative FACS plots of the three populations shown in (A). Numbers below FACS plots indicate frequencies of cells in each quadrant. (**C**) Quantification of pooled data of the relative number of Ki67$^+$Foxp3$^+$ Tregs. Gated on CD44$^+$ tetramer$^+$ T cells. Data are representative of four independent experiments; individual dots represent cells derived from individual mice.

sion and accumulation but rather reflected defective Treg differentiation or function.

*miR-17–92 regulates production of IL-10 by Foxp3$^+$ Tregs*

CD28-mediated costimulation is required for the production of the immunosuppressive cytokine IL-10 in Tregs, an effect that is enhanced by IL-2 (46). Because Treg-secreted IL-10 is a major mechanism of Treg-mediated control of EAE (25), we examined the role of miR-17–92 in IL-10 secretion by Tregs in the CNS at peak disease. Although IL-10 was readily detected in Tregs (CD4$^+$ CD25$^+$ or CD4$^+$GFP$^+$) isolated from control mice (Fig. 9A), Treg$^{\text{miR-17–92}-/-}$ mice had reduced frequencies of IL-10–producing Tregs (Fig. 9A, 9B). Because the number of Tregs was comparable in control and Treg$^{\text{miR-17–92}-/-}$ mice (Fig. 3C), a reduced frequency of IL-10–producing Tregs also means a reduced absolute number of IL-10–producing Tregs. The frequency of IL-10–producing control Tregs positively correlated with disease severity. In contrast, the relative number of IL-10–producing miR-17–92–deficient Tregs, independently of clinical score, was comparable to that in control mice with mild disease (Fig. 9C). The reduction of IL-10–producing Tregs was even more apparent in the Ag-specific Tregs (Fig. 9D, 9E), demonstrating that the reduced frequency of IL-10–producing Tregs was not a consequence of reduced Ag-specific Treg but rather most likely reflected defective differentiation into IL-10–producing effector Tregs (47).

## Discussion

Despite evidence of the overall importance of miRNAs as regulatory elements of Treg function and survival, very few individual miRNAs have been characterized in Tregs in vivo (5). Although *Dicer*, *Drosha*, and *Dgcr8* ablation in Tregs leads to spontaneous loss of tolerance and a scurfy-like disease (1–4), no single miRNA accounting for an equally dramatic loss of Treg function when ablated specifically in Treg has been found yet. The direct Foxp3 target bic/miR-155 facilitates IL-2 signaling and thus promotes Treg survival but is largely dispensable for Treg function (48, 49). miR-146a is required to suppress Th1-type inflammation in a high-stress setting, but its function under homeostatic conditions remains to be determined (50). In this study, we observed that a single miRNA cluster, miR-17–92, was upregulated during T cell activation in a CD28 costimulation–dependent manner and had a dramatic effect on the development of organ-specific autoimmunity. Specifically, miR-17–92 deficiency severely reduced the frequency of Ag-specific Tregs in LNs during priming as well as their quality in the effector tissue where miR-17–92 expression in Tregs was required for IL-10 production.

Like other miRNAs that are highly expressed in Tregs (e.g., miR-155), we observed that the miR-17–92 cluster is largely dispensable under homeostatic conditions. miRNAs are often considered "rheostats" or fine-tuners of mammalian gene expression as individual miRNAs only mildly regulate their hundreds of simultaneously targeted genes (35, 36). Accumulating observations suggest that miRNA rheostat function may only be revealed after a cell has to respond to a change in its environment (i.e., a specific stress) (37, 38, 51). In fact, most individual miRNAs (52) and even many miRNA families altogether (53) are dispensable under homeostatic conditions, indicating that a certain degree of fluctuation or imprecision of gene expression is well tolerated. In contrast, all components of a genetic network need to be optimally regulated during stress. Therefore, stress stimuli can reveal underappreciated miRNA functions (54).

T cell activation induces a specific stress response (17), and therefore, Ag challenge can serve as a model of a specific, temporally controlled stress stimulus in vivo. The prototypical costimulatory molecule CD28 promotes proliferation and survival but, in addition, induces metabolic changes that are not simply a consequence of T cell activation but are active and excessive processes anticipating increased energy needs ensuring that the activated cells can cope with the induced stress (18). Therefore, we used peptide–MHC tetramers to track Ag-specific (tetramer$^+$) Tregs arising during a major stress response in vivo (autoimmunity) comparing them to tetramer$^-$ cells in the same autoimmune setting. Of note, although the total Treg population was miR-17–92 deficient, the effect of miR-17–92 disruption was selectively observed in the MOG Ag-specific Tregs where it directly affected Treg numbers during activation. The selective defect in the tet-

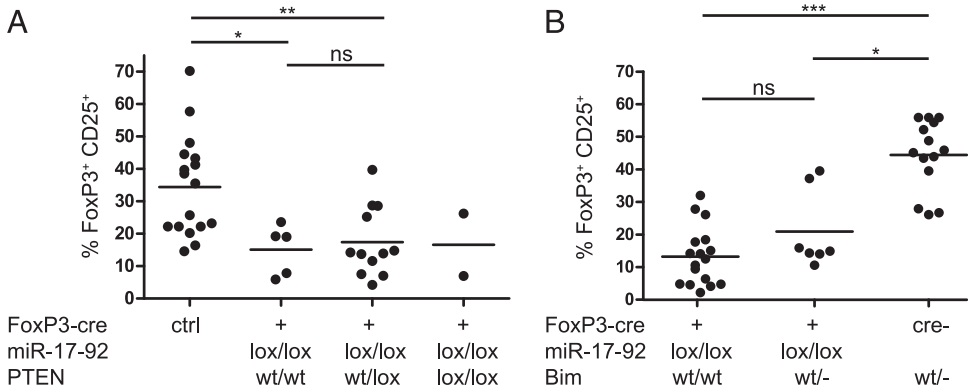


**FIGURE 6.** The frequency of miR-17–92–deficient Ag-specific Treg cannot be rescued by *Pten* deficiency or *Bim* heterozygosity. Analysis of frequencies of CD4$^+$CD44$^+$tetramer$^+$Foxp3$^+$CD25$^+$ Tregs of pooled MOG/CFA-primed d7 LNs and Spl. The same gating strategy was applied as shown in Fig. 4C and 4D. (**A** and **B**) Quantification of relative numbers of Foxp3$^+$CD25$^+$ Tregs among CD4$^+$CD44$^+$tetramer$^+$ cells. Genetic *Pten* rescue is shown in (A) and *Bim* rescue in (B). Pooled data are from at least six independent experiments. Individual dots represent individual mice. Cohorts in (A) and (B) are independent from each other and from mice shown in Fig. 4. Kruskal–Wallis test with post hoc Dunn's multiple comparison test: $p = 0.0029$ (A) and $p < 0.0001$ (B).

ramer$^+$ Treg likely reflects that Tregs receiving cognate MOG-MHC TCR stimulus were the most strongly activated ones (as reflected by increased CD25 levels compared with tetramer$^-$ Tregs) and therefore were more dependent on miR-17–92 than Tregs that were not or not fully activated (tetramer$^-$). Of note, some Treg$^{\text{miR-17–92}-/-}$ mice displayed a small percentage of Foxp3$^-$CD25$^+$ cells among the tetramer$^+$ cells. Additional studies including lineage-tracing mice are needed to clarify whether those represent unstable Tregs that lost Foxp3 or activated Tconvs displaying high CD25 expression.

We propose that in miRNA-deficient Tregs (1–4) combined functional defects (as a consequence of multiple miRNA deficiencies) result in a total breakdown of Treg function, stability, and survival leading to a scurfy-like Treg deficiency. In contrast, the loss of miR-17–92 results in more subtle and selective Treg defects that are essential during Ag priming and at the site of inflammation where cytokines, and Ag-driven signals are poised to disrupt or amplify Treg function (55, 56). In this regard, upon breaking of Treg tolerance and increasing autoreactive T cell activation, self-reactive Tregs become activated and expand in an attempt to control inflammation. The absence of the miR-17–92 cluster leads to an impairment of Ag-specific Tregs to accumulate at the site of Ag-priming and those that do accumulate lose their effector function as a result of an inability to produce IL-10, an immunoregulatory cytokine critical for the control of EAE. This reinforces a vicious cycle resulting in fulminant disease despite the presence of Foxp3$^+$ Tregs (1). In addition, the results demonstrated that miR-17–92 is an important component of the CD28 costimulatory program. Therefore, miR-17–92–mediated stress resistance likely plays an important role predominantly in those cells that receive proper activation signals by recognition of the cognate peptide–MHC in conjunction with a costimulatory signal from an activated APC. In contrast, Tregs, and possibly other T cells, recognizing only their peptide–MHC complex in the absence of a proper second signal including miR-17–92 regulation (e.g., on a nonactivated APC) are prone to die. It is important to note that miR-17–92 deficiency only mildly impaired T cell proliferation, and the phenotypic consequences cannot be fully

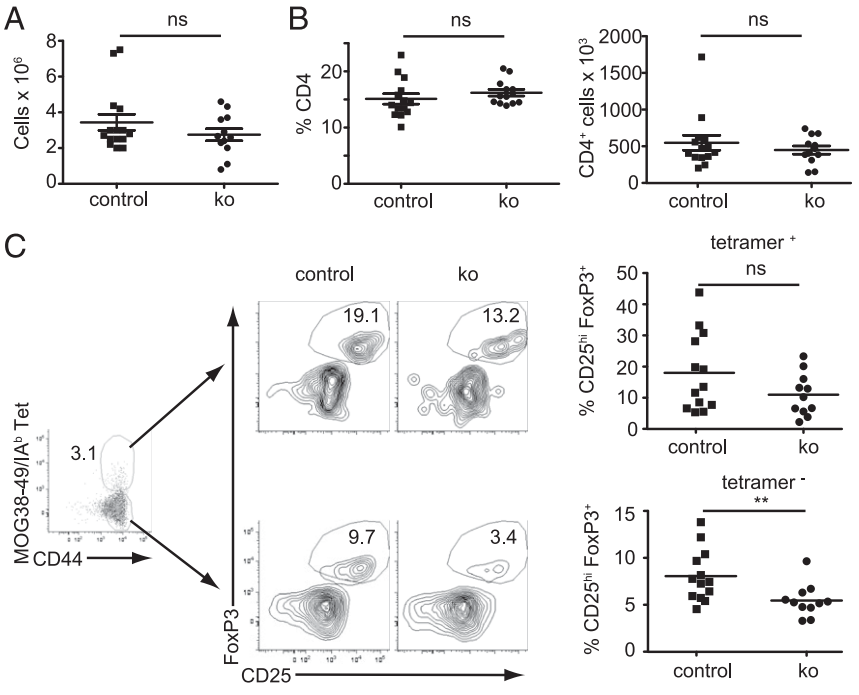


**FIGURE 7.** Normal numbers of Ag-specific Tregs in the CNS at peak disease. Lymphocytes isolated from CNS from mice with EAE score ≥ 1 at 15 d postpriming. (**A**) Total number of infiltrating cells. (**B**) Relative and absolute numbers of CD4$^+$ cells. Gated on live singlet CD8$^-$B220$^-$ CD11b$^-$CD11c$^-$ cells. (**C**) Representative FACS plots and quantification of Foxp3$^+$CD25$^{hi}$ Tregs in control and knockout (ko) mice. CD44$^+$tetramer$^+$ (*upper panel*) and CD44$^+$tetramer$^-$ (*lower panel*). Two-tailed Mann–Whitney tests: (A) $p = 0.4768$; (B) $p = 0.1262$ (relative) and $p = 0.0.8170$ (absolute) numbers; (C) tetramer$^+$, $p = 0.2025$; tetramer$^-$, $p = 0.0077$. Shown is pooled data from five independent experiments; dots represent cells derived from individual mice. The representative FACS plots showing the tetramer/CD44 gating is from a control mouse.

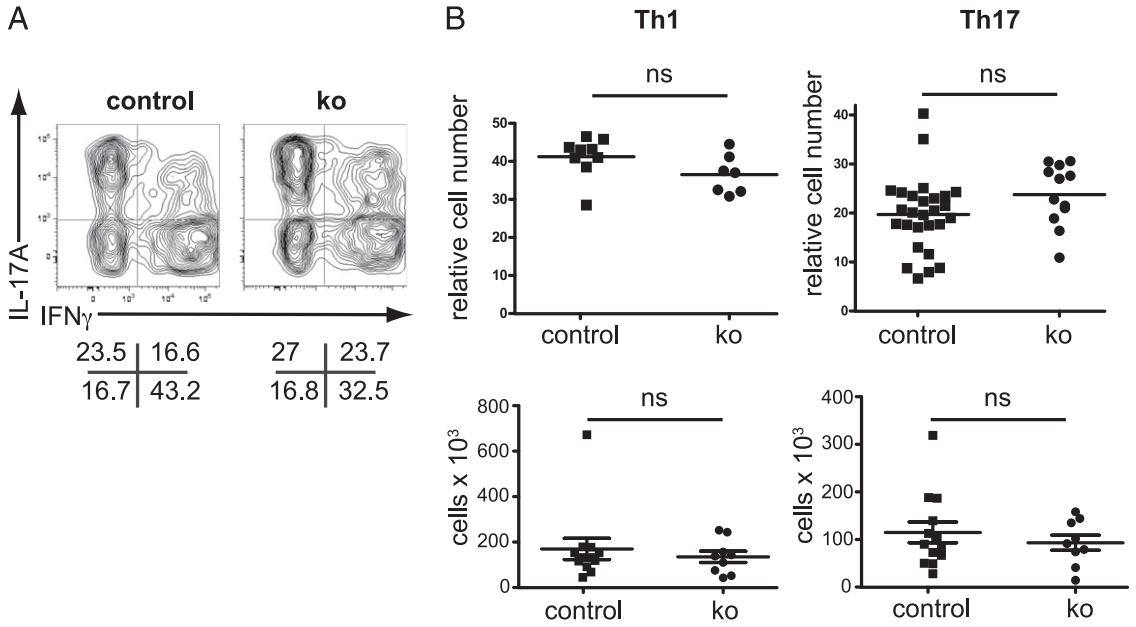


**FIGURE 8.** No detectable differences in Th1 and Th17 effector functions. Lymphocytes isolated from CNS from mice with EAE score ≥ 1 at 15 d postpriming. (**A**) Representative flow cytometry plots. Numbers below graphs represent frequencies of cells in each quadrant. (**B**) Quantification of relative and absolute numbers of Th1 (live singlet $CD4^+IFN\gamma^+IL\text{-}17A^-$) and Th17 (live singlet $CD4^+IFN\gamma^-IL\text{-}17A^+$) cells as defined in (A). Pooled data from five or more experiments; dots represent cells derived from individual mice. Two-tailed Mann–Whitney tests: (B) $p = 0.1142$ (relative number of Th1); $p = 0.0726$ (relative number of Th17); $p = 0.8590$ (absolute number of Th1); $p = 0.7894$ (absolute number of Th17).

accounted for by miR-17–92 control of PTEN or BIM pathways. Although normal proliferation but reduced cell numbers suggest cell death, we were not able to define which cell death pathway was activated. Despite our findings that neither *Pten* deficiency nor *Bim* heterozygosity were sufficient to restore Treg survival in the absence of miR-17–92, it is possible that their repression is functionally relevant in other cell types for other functions such as IL-10 secretion or through cooperation with other targets. As an example, during follicular Th cell differentiation *Pten* is a minor functionally relevant target (34). Likewise, because the miR-17–92 cluster is redundant, it is possible that the paralog clusters miR-106a–363 and miR-106b–25 compensated to maintain proliferative capacity. However, in our model, the paralog clusters did not compensate for loss of miR-17–92 to produce IL-10.

Requirements for costimulation are cell-type and differentiation stage dependent, and costimulation can have different or even opposing roles for an immune response depending on the cell type that is stimulated (19). In this regard, it is interesting to note that the expression of the miR-17–92 cluster opposes TGF-β–mediated iTreg induction in vitro (10). In contrast, we observed just the opposite in natural Tregs, namely, that the expression of miR-17–92 is critical in maintaining this subset during an autoimmune response in vivo. This conundrum may be explained by the observation that strong costimulation has distinct effects on natural versus adaptive Treg induction wherein the former has a critical requirement for maximal TCR/costimulation signaling, whereas the latter subset of Tregs appear to develop and are maintained by a more limited TCR/CD28 signal (57). Absence of miR-17–92, leading to an attenuated CD28 signal, would therefore result in increased TGF-β–mediated iTreg induction (10). In addition, increased sensitivity to TGF-β (10, 58) in combination with reduced costimulation likely cooperates to promote Foxp3 induction in miR-17–92–deficient T cells. Future studies will need to address how miR-17–92 differentially affects natural versus adaptive Tregs and whether miR-17–92 has further opposing functions in other cell types or functional states, possibly because of other factors such as retinoic acid (57) or cytokines.

During the course of EAE, Treg-secreted IL-10 is key to the control of disease as adoptively transferred IL-10–deficient Tregs fail to suppress EAE (25). The production of IL-10 by Tregs is dynamic, peaking during recovery where almost half of the Tregs in the CNS produce IL-10 (33). Of note, IL-10 production by Tregs is tissue dependent because $CD4^+CD25^+$ cells in LNs produce much less IL-10 than their CNS Treg counterparts isolated from the same mice (39). Thus, CNS Tregs likely adapt to their environment by sensing a signal such as a cytokine absent in the LN and respond with IL-10 secretion. Supporting this notion, we observed a positive correlation between clinical score and frequency of IL-10–producing Tregs in control mice, suggesting a feed forward loop in response to inflammation. The higher frequency of $IL\text{-}10^+$ Tregs among Ag-specific Tregs compared with $tetramer^-$ Tregs most likely represents activation of Ag-specific Tregs (reflected by higher CD25 expression). There are multiple scenarios that might explain why miR-17–92–deficient Tregs produce less IL-10: 1) miR-17–92 might be required for IL-10 production per se; 2) miR-17–92 could regulate the positive feedback loop and/or; 3) miR-17–92 could be required for the differentiation of Tregs into IL-10–producing effector Treg (47). We have recently demonstrated that miR-17–92 plays a minor role promoting proliferation but is required for proper follicular Th cell differentiation. Furthermore, follicular Th cell but not polyclonal Treg numbers correlated strongly with miR-17–92 dose (34). Importantly, follicular regulatory T cells are enriched in IL-10 mRNA compared with conventional Tregs (59). In analogy, we hypothesize that the most likely explanation for the IL-10 defect is impaired differentiation. Because differentiation into IL-10–producing effector Tregs in tissues is mediated by Blimp-1 and IFN regulatory factor 4, future studies will need to address whether miR-17–92 regulates these genes directly or indirectly (47). It remains to be tested whether miR-17–92 regulates IL-10 pro-

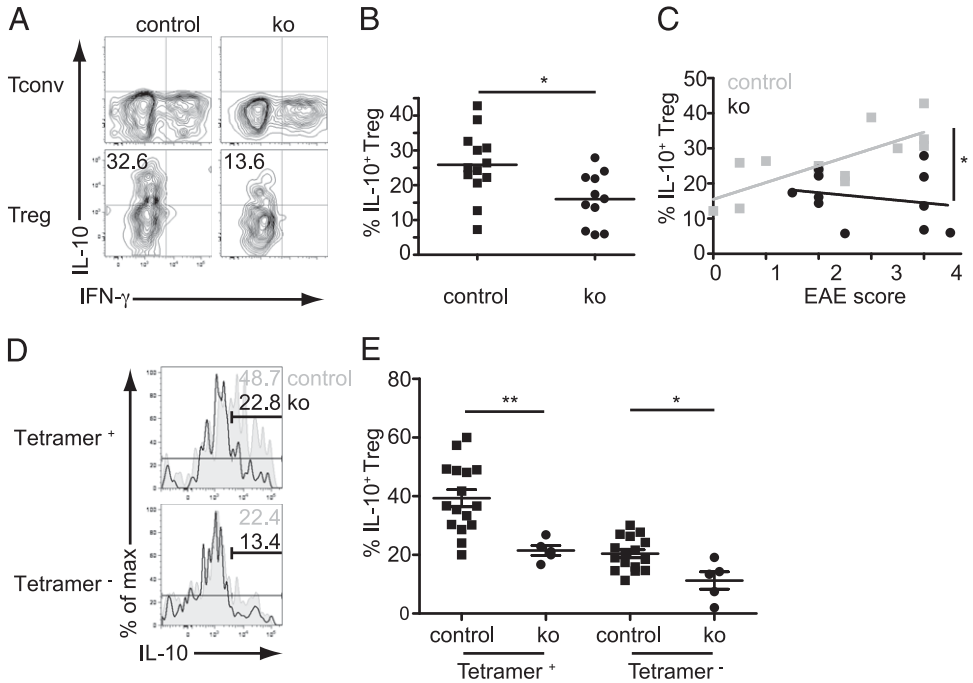


**FIGURE 9.** miR-17–92 regulates production of IL-10 by Foxp3$^+$ Tregs. Lymphocytes were isolated from CNS 15 d post-MOG/CFA priming. Representative FACS plots (**A**) and quantification (**B**) of the frequency of CD4$^+$CD25$^+$ Treg secreting IL-10. (**C**) Relative number of IL-10$^+$ Tregs (CD4$^+$CD25$^+$) as a function of clinical EAE score. (**D**) Representative histogram overlays of relative number of IL-10$^+$ Tregs (CD4$^+$CD25$^+$) among MOG38–49/I-A$^b$ tetramer$^+$ and tetramer$^-$ cells. IL-10 gating was based on CD4$^+$CD25$^-$ Tconvs (IL-10 negative) as shown in (A). Numbers indicate the percentage of IL-10$^+$ cells. (**E**) Quantification of (D). Shown is pooled data from five (A–C) and three (D, E) independent experiments; individual symbols represent cells derived from individual mice (B, C, E); error bars represent SEM. Two-tailed Mann–Whitney *U* test: $p = 0.0117$ (B), $p = 0.0038$ (E, tetramer$^+$), $p = 0.0149$ (E, tetramer$^-$). Linear regression analysis (C): $p = 0.01357$ that slopes of control and ko are different. Data in (D) and (E) are independent from data in (A), (B), and (C).

duction in other cell types such as Foxp3$^-$ Tr1 cells or whether this function is unique to Tregs.

It should be noted that we still observed reduced IL-10 production in tetramer$^-$ cells, which are the majority of CD4$^+$ T cells. Thus, either all Tregs may be affected (not only the tetramer$^+$ ones) or other Ag-specific Tregs (not reactive with the tetramers) are also affected. However, distinguishing these possibilities is difficult because tetramer$^-$ Tregs are a heterogeneous population where the Ag–nonspecific Tregs recruited by inflammation-induced chemoattractants cannot be distinguished easily from Ag-specific Tregs recognizing other epitopes than those surveyed by the use of the MOG peptide tetramer. Nevertheless, this finding is in contrast to Treg accumulation in the LN where the absence of miR-17–92 led to a selective defect in tetramer$^+$ but not tetramer$^-$ Tregs.

Finally, it is noteworthy that miR-17–92–deficient Tregs were still able to control effector T cell responses in the CNS numerically. One possible explanation is that the reduced number of Ag-specific Tregs during priming led to uncontrolled priming of effector T cells (Teffs). Because effector T cell numbers were not increased in Treg$^{\text{miR-17–92}-/-}$ mice, this could mean that Teff actually left the LN prematurely as suggested by the paper by Davidson and Shevach (60) that demonstrates that Tregs control Teff LN emigration in EAE. Whether increased CD69 on miR-17–92–deficient Tregs compromised Treg emigration and thus further contributed to disease remains to be tested (61). If premature Teff egress from LN did occur, it was not sufficient to cause early onset disease in most Treg$^{\text{miR-17–92}-/-}$ mice. Thus, the normal numbers of total CD4$^+$, Th1, and Th17 cells in the CNS of Treg$^{\text{miR-17–92}-/-}$ mice suggest that the quality of the effector response is altered. Alternatively, it is possible that the restimulation with PMA/ionomycin masked dysregulation of subsets of self-reactive Teff such as T cells reactive against MOG or other self-peptides. Further studies are needed to uncover whether increased disease severity was a result of unrestrained Teff function, impaired Treg migration/location, or impaired suppression of cells other than Th1 or Th17.

In summary, we propose that miR-17–92 controls multiple important Treg-intrinsic functions during several phases of Treg differentiation and/or function that may be controlled by non-overlapping miR-17–92 targets. During Ag-priming miR-17–92 is induced by CD28 costimulation supporting accumulation of Ag-specific Tregs, most likely by promoting survival. Later, once migrated into the effector tissue, miR-17–92 mediates sensing of some as yet unidentified inflammatory signal and/or differentiation into IL-10–producing Tregs. Because miRNAs target hundreds of genes, it is conceivable that miR-17–92 controls other functions as well. If the elevated CD69 levels are functionally relevant, miR-17–92 also might control migration and tissue location of Tregs. In addition, the mildly reduced CTLA-4 could further compromise Treg function. Therefore, the exacerbated EAE is unlikely to be exclusively because of the two described defects, but accumulation of Ag-specific Tregs and IL-10 production are likely important contributors.

## Acknowledgments

We thank Abul Abbas, Mark Ansel, and Robert Blelloch for critically reading the manuscript; Samantha Bailey-Bucktrout for a thorough introduction to EAE and MOG–MHC tetramer technology; members of the Bluestone, Abbas, and Anderson laboratories; Mark Ansel, Mike McManus, and the UCSF miRNA in lymphocyte group for scientific discussions; Dorothy Fuentes for expert animal husbandry; Duy Le for outstanding help with

genotyping; Navdeep Grewal and Una Fan for help with histology; Shuwei Jiang and Mike Lee for cell sorting; Haopeng Wang for providing an optimized IL-10 staining protocol; the Emory National Institutes of Health Tetramer facility for tetramers (http://tetramer.yerkes.emory.edu/facility/facility); Chris Barker and Yanxia Hao from the UCSF Gladstone Genomics Core for miRNA array; and Dr. Tak Mak (University Health Network, Toronto, ON, Canada) for PTEN$^{lox}$ mice.

## Disclosures

The authors have no financial conflicts of interest.

## References

1. Zhou, X., L. T. Jeker, B. T. Fife, S. Zhu, M. S. Anderson, M. T. McManus, and J. A. Bluestone. 2008. Selective miRNA disruption in Treg cells leads to uncontrolled autoimmunity. *J. Exp. Med.* 205: 1983–1991.
2. Chong, M. M., J. P. Rasmussen, A. Y. Rudensky, and D. R. Littman. 2008. The RNAseIII enzyme Drosha is critical in T cells for preventing lethal inflammatory disease. *J. Exp. Med.* 205: 2005–2017.
3. Liston, A., L. F. Lu, D. O'Carroll, A. Tarakhovsky, and A. Y. Rudensky. 2008. Dicer-dependent microRNA pathway safeguards regulatory T cell function. *J. Exp. Med.* 205: 1993–2004.
4. Jeker, L. T., X. Zhou, R. Blelloch, and J. A. Bluestone. 2013. DGCR8-mediated production of canonical micrornas is critical for regulatory T cell function and stability. *PLoS One* DOI: 10.1371/journal.pone.0066282.
5. Jeker, L. T., and J. A. Bluestone. 2013. MicroRNA regulation of T-cell differentiation and function. *Immunol. Rev.* 253: 65–81.
6. He, L., J. M. Thomson, M. T. Hemann, E. Hernando-Monge, D. Mu, S. Goodson, S. Powers, C. Cordon-Cardo, S. W. Lowe, G. J. Hannon, and S. M. Hammond. 2005. A microRNA polycistron as a potential human oncogene. *Nature* 435: 828–833.
7. Ventura, A., A. G. Young, M. M. Winslow, L. Lintault, A. Meissner, S. J. Erkeland, J. Newman, R. T. Bronson, D. Crowley, J. R. Stone, et al. 2008. Targeted deletion reveals essential and overlapping functions of the miR-17 through 92 family of miRNA clusters. *Cell* 132: 875–886.
8. Mendell, J. T. 2008. miRiad roles for the miR-17-92 cluster in development and disease. *Cell* 133: 217–222.
9. de Pontual, L., E. Yao, P. Callier, L. Faivre, V. Drouin, S. Cariou, A. Van Haeringen, D. Geneviève, A. Goldenberg, M. Oufadem, et al. 2011. Germline deletion of the miR-17~92 cluster causes skeletal and growth defects in humans. *Nat. Genet.* 43: 1026–1030.
10. Jiang, S., C. Li, V. Olive, E. Lykken, F. Feng, J. Sevilla, Y. Wan, L. He, and Q. J. Li. 2011. Molecular dissection of the miR-17-92 cluster's critical dual roles in promoting Th1 responses and preventing inducible Treg differentiation. *Blood* 118: 5487–5497.
11. Wu, T., A. Wieland, K. Araki, C. W. Davis, L. Ye, J. S. Hale, and R. Ahmed. 2012. Temporal expression of microRNA cluster miR-17-92 regulates effector and memory CD8$^+$ T-cell differentiation. *Proc. Natl. Acad. Sci. USA* 109: 9965–9970.
12. Barski, A., R. Jothi, S. Cuddapah, K. Cui, T. Y. Roh, D. E. Schones, and K. Zhao. 2009. Chromatin poises miRNA- and protein-coding genes for expression. *Genome Res.* 19: 1742–1751.
13. Sandberg, R., J. R. Neilson, A. Sarma, P. A. Sharp, and C. B. Burge. 2008. Proliferating cells express mRNAs with shortened 3′ untranslated regions and fewer microRNA target sites. *Science* 320: 1643–1647.
14. Xiao, C., L. Srinivasan, D. P. Calado, H. C. Patterson, B. Zhang, J. Wang, J. M. Henderson, J. L. Kutok, and K. Rajewsky. 2008. Lymphoproliferative disease and autoimmunity in mice with increased miR-17-92 expression in lymphocytes. *Nat. Immunol.* 9: 405–414.
15. Tufekci, K. U., M. G. Oner, S. Genc, and K. Genc. 2011. MicroRNAs and multiple sclerosis. *Autoimmune Dis.* 2011: 807426.
16. Junker, A., R. Hohlfeld, and E. Meinl. 2011. The emerging role of microRNAs in multiple sclerosis. *Nat. Rev. Neurol.* 7: 56–59.
17. Scheu, S., D. B. Stetson, R. L. Reinhardt, J. H. Leber, M. Mohrs, and R. M. Locksley. 2006. Activation of the integrated stress response during T helper cell differentiation. *Nat. Immunol.* 7: 644–651.
18. Frauwirth, K. A., J. L. Riley, M. H. Harris, R. V. Parry, J. C. Rathmell, D. R. Plas, R. L. Elstrom, C. H. June, and C. B. Thompson. 2002. The CD28 signaling pathway regulates glucose metabolism. *Immunity* 16: 769–777.
19. Bour-Jordan, H., J. H. Esensten, M. Martinez-Llordella, C. Penaranda, M. Stumpf, and J. A. Bluestone. 2011. Intrinsic and extrinsic control of peripheral T-cell tolerance by costimulatory molecules of the CD28/B7 family. *Immunol. Rev.* 241: 180–205.
20. Bour-Jordan, H., and J. A. Bluestone. 2009. Regulating the regulators: costimulatory signals control the homeostasis and function of regulatory T cells. *Immunol. Rev.* 229: 41–66.
21. Salomon, B., D. J. Lenschow, L. Rhee, N. Ashourian, B. Singh, A. Sharpe, and J. A. Bluestone. 2000. B7/CD28 costimulation is essential for the homeostasis of the CD4$^+$CD25$^+$ immunoregulatory T cells that control autoimmune diabetes. *Immunity* 12: 431–440.
22. Buckler, J. L., P. T. Walsh, P. M. Porrett, Y. Choi, and L. A. Turka. 2006. Cutting edge: T cell requirement for CD28 costimulation is due to negative regulation of TCR signals by PTEN. *J. Immunol.* 177: 4262–4266.
23. Tang, Q., and J. A. Bluestone. 2008. The Foxp3$^+$ regulatory T cell: a jack of all trades, master of regulation. *Nat. Immunol.* 9: 239–244.
24. Rubtsov, Y. P., J. P. Rasmussen, E. Y. Chi, J. Fontenot, L. Castelli, X. Ye, P. Treuting, L. Siewe, A. Roers, W. R. Henderson, Jr., et al. 2008. Regulatory T cell-derived interleukin-10 limits inflammation at environmental interfaces. *Immunity* 28: 546–558.
25. Zhang, X., D. N. Koldzic, L. Izikson, J. Reddy, R. F. Nazareno, S. Sakaguchi, V. K. Kuchroo, and H. L. Weiner. 2004. IL-10 is involved in the suppression of experimental autoimmune encephalomyelitis by CD25$^+$CD4$^+$ regulatory T cells. *Int. Immunol.* 16: 249–256.
26. Putnam, A. L., T. M. Brusko, M. R. Lee, W. Liu, G. L. Szot, T. Ghosh, M. A. Atkinson, and J. A. Bluestone. 2009. Expansion of human regulatory T-cells from patients with type 1 diabetes. *Diabetes* 58: 652–662.
27. Moltzahn, F., A. B. Olshen, L. Baehner, A. Peek, L. Fong, H. Stöppler, J. Simko, J. F. Hilton, P. Carroll, and R. Blelloch. 2011. Microfluidic-based multiplex qRT-PCR identifies diagnostic and prognostic microRNA signatures in the sera of prostate cancer patients. *Cancer Res.* 71: 550–560.
28. Suzuki, A., M. T. Yamaguchi, T. Ohteki, T. Sasaki, T. Kaisho, Y. Kimura, R. Yoshida, A. Wakeham, T. Higuchi, M. Fukumoto, et al. 2001. T cell-specific loss of Pten leads to defects in central and peripheral tolerance. *Immunity* 14: 523–534.
29. Bouillet, P., D. Metcalf, D. C. Huang, D. M. Tarlinton, T. W. Kay, F. Köntgen, J. M. Adams, and A. Strasser. 1999. Proapoptotic Bcl-2 relative Bim required for certain apoptotic responses, leukocyte homeostasis, and to preclude autoimmunity. *Science* 286: 1735–1738.
30. Tang, Q., K. J. Henriksen, M. Bi, E. B. Finger, G. Szot, J. Ye, E. L. Masteller, H. McDevitt, M. Bonyhadi, and J. A. Bluestone. 2004. In vitro-expanded antigen-specific regulatory T cells suppress autoimmune diabetes. *J. Exp. Med.* 199: 1455–1465.
31. Melton, A. C., S. L. Bailey-Bucktrout, M. A. Travis, B. T. Fife, J. A. Bluestone, and D. Sheppard. 2010. Expression of $\alpha_v\beta_8$ integrin on dendritic cells regulates Th17 cell development and experimental autoimmune encephalomyelitis in mice. *J. Clin. Invest.* 120: 4436–4444.
32. Moon, J. J., H. H. Chu, M. Pepper, S. J. McSorley, S. C. Jameson, R. M. Kedl, and M. K. Jenkins. 2007. Naive CD4$^+$ T cell frequency varies for different epitopes and predicts repertoire diversity and response magnitude. *Immunity* 27: 203–213.
33. Korn, T., J. Reddy, W. Gao, E. Bettelli, A. Awasthi, T. R. Petersen, B. T. Bäckström, R. A. Sobel, K. W. Wucherpfennig, T. B. Strom, et al. 2007. Myelin-specific regulatory T cells accumulate in the CNS but fail to control autoimmune inflammation. *Nat. Med.* 13: 423–431.
34. Baumjohann, D., R. Kageyama, J. M. Clingan, M. M. Morar, S. Patel, D. de Kouchkovsky, O. Bannard, J. A. Bluestone, M. Matloubian, K. M. Ansel, and L. T. Jeker. 2013. The microRNA cluster miR-17~92 promotes TFH cell differentiation and represses subset-inappropriate gene expression. *Nat. Immunol.* DOI: 10.1038/ni.2642.
35. Selbach, M., B. Schwanhäusser, N. Thierfelder, Z. Fang, R. Khanin, and N. Rajewsky. 2008. Widespread changes in protein synthesis induced by microRNAs. *Nature* 455: 58–63.
36. Baek, D., J. Villén, C. Shin, F. D. Camargo, S. P. Gygi, and D. P. Bartel. 2008. The impact of microRNAs on protein output. *Nature* 455: 64–71.
37. Leung, A. K., and P. A. Sharp. 2007. microRNAs: a safeguard against turmoil? *Cell* 130: 581–585.
38. Leung, A. K., and P. A. Sharp. 2010. MicroRNA functions in stress responses. *Mol. Cell* 40: 205–215.
39. McGeachy, M. J., L. A. Stephens, and S. M. Anderton. 2005. Natural recovery and protection from autoimmune encephalomyelitis: contribution of CD4$^+$ CD25$^+$ regulatory cells within the central nervous system. *J. Immunol.* 175: 3025–3032.
40. Schmidt-Supprian, M., and K. Rajewsky. 2007. Vagaries of conditional gene targeting. *Nat. Immunol.* 8: 665–668.
41. Zhang, N., and M. J. Bevan. 2010. Dicer controls CD8$^+$ T-cell activation, migration, and survival. *Proc. Natl. Acad. Sci. USA* 107: 21629–21634.
42. Friedman, R. C., K. K. Farh, C. B. Burge, and D. P. Bartel. 2009. Most mammalian mRNAs are conserved targets of microRNAs. *Genome Res.* 19: 92–105.
43. Malek, T. R., and A. L. Bayer. 2004. Tolerance, not immunity, crucially depends on IL-2. *Nat. Rev. Immunol.* 4: 665–674.
44. Barron, L., H. Dooms, K. K. Hoyer, W. Kuswanto, J. Hofmann, W. E. O'Gorman, and A. K. Abbas. 2010. Cutting edge: mechanisms of IL-2-dependent maintenance of functional regulatory T cells. *J. Immunol.* 185: 6426–6430.
45. Strasser, A. 2005. The role of BH3-only proteins in the immune system. *Nat. Rev. Immunol.* 5: 189–200.
46. Park, S. G., R. Mathur, M. Long, N. Hosh, L. Hao, M. S. Hayden, and S. Ghosh. 2010. T regulatory cells maintain intestinal homeostasis by suppressing γδ T cells. *Immunity* 33: 791–803.
47. Cretney, E., A. Xin, W. Shi, M. Minnich, F. Masson, M. Miasari, G. T. Belz, G. K. Smyth, M. Busslinger, S. L. Nutt, and A. Kallies. 2011. The transcription factors Blimp-1 and IRF4 jointly control the differentiation and function of effector regulatory T cells. *Nat. Immunol.* 12: 304–311.
48. Lu, L. F., T. H. Thai, D. P. Calado, A. Chaudhry, M. Kubo, K. Tanaka, G. B. Loeb, H. Lee, A. Yoshimura, K. Rajewsky, and A. Y. Rudensky. 2009. Foxp3-dependent microRNA155 confers competitive fitness to regulatory T cells by targeting SOCS1 protein. *Immunity* 30: 80–91.
49. Kohlhaas, S., O. A. Garden, C. Scudamore, M. Turner, K. Okkenhaug, and E. Vigorito. 2009. Cutting edge: the Foxp3 target miR-155 contributes to the development of regulatory T cells. *J. Immunol.* 182: 2578–2582.

50. Lu, L. F., M. P. Boldin, A. Chaudhry, L. L. Lin, K. D. Taganov, T. Hanada, A. Yoshimura, D. Baltimore, and A. Y. Rudensky. 2010. Function of miR-146a in controlling Treg cell-mediated regulation of Th1 responses. *Cell* 142: 914–929.
51. Jeker, L. T., and J. A. Bluestone. 2010. Small RNA regulators of T cell-mediated autoimmunity. *J. Clin. Immunol.* 30: 347–357.
52. Miska, E. A., E. Alvarez-Saavedra, A. L. Abbott, N. C. Lau, A. B. Hellman, S. M. McGonagle, D. P. Bartel, V. R. Ambros, and H. R. Horvitz. 2007. Most *Caenorhabditis elegans* microRNAs are individually not essential for development or viability. *PLoS Genet.* 3: e215.
53. Alvarez-Saavedra, E., and H. R. Horvitz. 2010. Many families of *C. elegans* microRNAs are not essential for development or viability. *Curr. Biol.* 20: 367–373.
54. Li, X., J. J. Cassidy, C. A. Reinke, S. Fischboeck, and R. W. Carthew. 2009. A microRNA imparts robustness against environmental fluctuation during development. *Cell* 137: 273–282.
55. Zhou, X., S. Bailey-Bucktrout, L. T. Jeker, and J. A. Bluestone. 2009. Plasticity of $CD4^+$ $FoxP3^+$ T cells. *Curr. Opin. Immunol.* 21: 281–285.
56. Chaudhry, A., R. M. Samstein, P. Treuting, Y. Liang, M. C. Pils, J. M. Heinrich, R. S. Jack, F. T. Wunderlich, J. C. Brüning, W. Müller, and A. Y. Rudensky. 2011. Interleukin-10 signaling in regulatory T cells is required for suppression of Th17 cell-mediated inflammation. *Immunity* 34: 566–578.
57. Benson, M. J., K. Pino-Lagos, M. Rosemblatt, and R. J. Noelle. 2007. All-trans retinoic acid mediates enhanced T reg cell growth, differentiation, and gut homing in the face of high levels of co-stimulation. *J. Exp. Med.* 204: 1765–1774.
58. Mestdagh, P., A. K. Boström, F. Impens, E. Fredlund, G. Van Peer, P. De Antonellis, K. von Stedingk, B. Ghesquière, S. Schulte, M. Dews, et al. 2010. The miR-17-92 microRNA cluster regulates multiple components of the TGF-β pathway in neuroblastoma. *Mol. Cell* 40: 762–773.
59. Linterman, M. A., W. Pierson, S. K. Lee, A. Kallies, S. Kawamoto, T. F. Rayner, M. Srivastava, D. P. Divekar, L. Beaton, J. J. Hogan, et al. 2011. $Foxp3^+$ follicular regulatory T cells control the germinal center response. *Nat. Med.* 17: 975–982.
60. Davidson, T. S., and E. M. Shevach. 2011. Polyclonal Treg cells modulate T effector cell trafficking. *Eur. J. Immunol.* 41: 2862–2870.
61. Shiow, L. R., D. B. Rosen, N. Brdicková, Y. Xu, J. An, L. L. Lanier, J. G. Cyster, and M. Matloubian. 2006. CD69 acts downstream of interferon-α/β to inhibit S1P1 and lymphocyte egress from lymphoid organs. *Nature* 440: 540–544.

**Supplemental Figure 1**

**miR-17-92 cluster induction in human naive T cells depends on CD28 costimulation**

Microarray analysis of miRNA expression in human $CD4^+CD45RA^+$ T cells stimulated for 24h with anti-CD3 alone or a combination of anti-CD3 and anti-CD28. Data are pooled from three experiments.

**Supplemental Figure 2**

**CD69 is a likely direct target of miR-17-92**

Flow cytometry based phenotypic characterization of miR-17-92-deficient Treg. Pooled lymph node (LN) and spleen from mice immunized with MOG35-55/CFA were analyzed 7 days post priming. Gated on live $CD4^+Foxp3^-$ (Tconv) or $CD4^+Foxp3^+$ (Treg). The mean fluorescence intensity (MFI) was normalized due to inter-experimental variability. Shown are pooled data from 4 (CD127, GITR, CD103, CTLA-4, CD69) and 3 (Neuropilin-1) independent experiments; error bars represent SEM; symbols represent individual mice. Two-tailed Mann-Whitney test was used to compare control and ko for Tconv and Treg separately: $p=0.0348$ (E, Treg), $p<0.0001$ (F, Treg).

**Supplemental Figure 1**



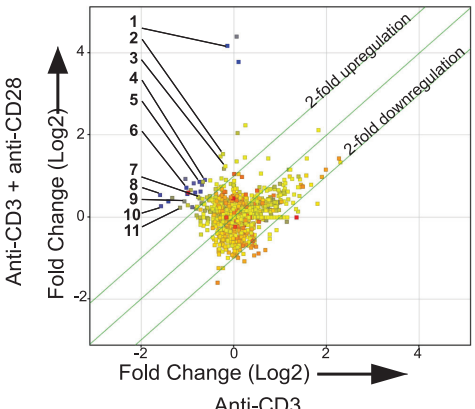


1. hsa-miR-155
2. hsa-miR-18a
3. hsa-miR-18b
4. hsa-miR-106a
5. hsa-miR-17
6. hsa-miR-20b
7. hsa-miR-106b
8. hsa-miR-20a
9. hsa-miR-19b
10. hsa-miR-19a
11. hsa-miR-93

# Supplemental Figure 2

De Kouchkovsky et al.